Received 7 June 2022; revised 16 August 2022 and 7 September 2022; accepted 7 September 2022. Date of publication 5 October 2022; date of current version 6 January 2023.

Digital Object Identifier 10.1109/JMW.2022.3206715

Flexible Lumped Microwave Passive Components and Filters on Cellulose Nanofibril Substrates

SHUOYANG QIU [1], HUILONG ZHANG [1,2], QIANGU YAN [3], LINDA KATEHI [4], SHAOQIN GONG [2,5], ZHIYONG CAI [3], AND ZHENQIANG MA [1,6,7]

(Regular Paper)

[1] Department of Electrical and Computer Engineering, University of Wisconsin – Madison, Madison, WI 53706 USA
[2] Wisconsin Institute for Discovery, University of Wisconsin – Madison, Madison, WI 53706 USA
[3] Forest Products Laboratory, USDA Forest Service, Madison, WI 53726 USA
[4] Department of Electrical and Computer Engineering, Texas A&M University, College Station, TX 77843 USA
[5] Department of Biomedical Engineering, University of Wisconsin – Madison, Madison, WI 53706 USA
[6] Department of Materials Science and Engineering, University of Wisconsin – Madison, Madison, WI 53706 USA
[7] Department of Engineering Physics, University of Wisconsin – Madison, Madison, WI 53706 USA

CORRESPONDING AUTHORS: Zhiyong Cai; Zhenqiang Ma (e-mail: Zhiyong.cai@usda.gov; mazq@engr.wisc.edu).
(Shuoyang Qiu and Huilong Zhang contributed equally to this work.)

This work was supported by the China Scholarship Council.
This article has supplementary downloadable material available at https://doi.org/10.1109/JMW.2022.3206715, provided by the authors.

ABSTRACT Cellulose nanofibril (CNF) substrates that are inexpensive, biodegradable, and quickly incinerable, are potential substrates for disposable RF applications. In this paper, high-performance flexible microwave lumped elements and filters fabricated on flexible CNF substrates are reported. A spiral inductor with a resonance frequency of 29.8 GHz and quality (Q) factor of 8.5 and a metal-insulator-metal (MIM) capacitor with a resonance frequency of 45 GHz and Q factor of 85.2 were achieved in a 200 μm thick CNF substrate. Meanwhile, the inductor and capacitor exhibit outstanding mechanical bendability, that is negligible performance changes were observed when they were bent to a radius as small as 15 mm. Based on the spiral inductor and MIM capacitor, a 5-GHz band-stop filter and a 4 GHz band-pass filter with excellent mechanical bendability were further demonstrated on the CNF substrate. These results indicate the potential of using CNF as substrates for broader microwave applications.

INDEX TERMS Cellulose nanofibril, flexible electronics, microwave applications, radio-frequency inductor-capacitor and filters.

I. INTRODUCTION

Microwave electronics have been experiencing significant evolutions over the last few decades, from bulky vacuum tube-based devices, and printed circuit boards (PCB), to compact monolithic microwave integrated circuits (MMIC). In the recent decade, microwave electronics in mechanically flexible/stretchable form have emerged and experienced rapid development to address new requirements from emerging wearable devices, which cannot be easily addressed by conventional rigid microwave electronics [1]. To achieve mechanical flexible electronics, bendable substrates with excellent microwave properties including low resistive loss and low tangent loss are required, in addition to bendable semiconductors materials. In the past decades, various polymer-based materials have been exploited for the substrate of flexible microwave electronics, including polyethylene terephthalate (PET), Kapton, polyethylene naphthalate (PEN), etc. These materials are inexpensive and have outstanding electrical properties at microwave frequency. Flexible microwave components like flexible capacitors and inductors have been demonstrated on these flexible substrates using different fabrication techniques. Sun et al. demonstrated a flexible inductor using spin-cast SU8 as an intermetal insulating layer and a flexible MIM capacitor with evaporated 200 nm SiO and TiO2

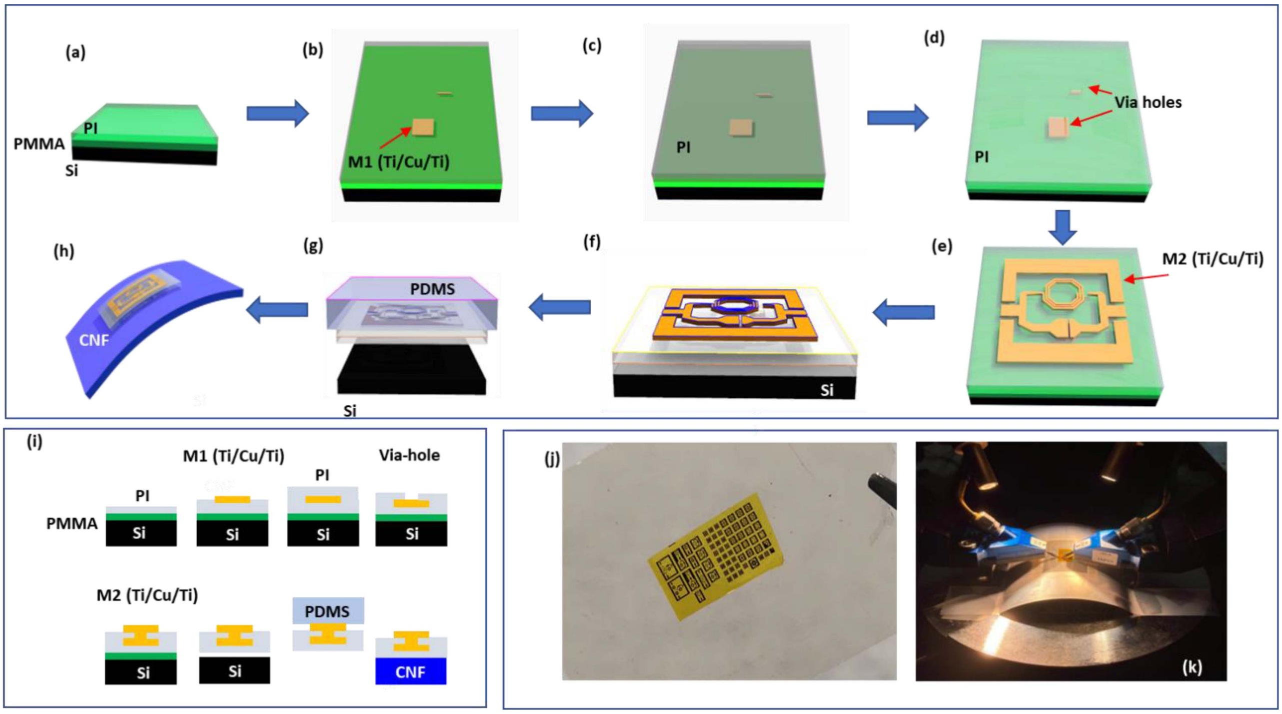

FIGURE 1. Illustration of the fabrication process flow for flexible inductors/capacitors and filters on CNF substrates. (a) PMMA and PI layers were spin-coated on Si substrate. (b) M1 (Ti/Cu/Ti) was evaporated on Si/PMMA/PI substrate to form the bottom electrode of capacitors and lower lead metal of spiral inductors. (c) A thick PI layer was deposited to encapsulate the M1 layer. (d) A hard mask was formed with Al using the electron-beam evaporator via a lift-off process. An anisotropic reactive ion plasma etching of encapsulated PI to define the via holes on the PI layer. (e) M2 metal layer (Ti/Cu/Ti) was evaporated to form the spiral metals of inductors and interconnects for filters. (f) PMMA layer was undercut using boiled acetone. (g) Devices were picked up by PDMS from the handling Si substrate. (h) Devices were transferred to a CNF substrate with spin-coated SU-8 as the adhesion layer. (i) The simplified cross-sectional view of the fabrication process flow. (j) An optical image of the fabricated L, C, and L-C filter array on a CNF substrate. (k) Flexible inductors/capacitors and filters on CNF substrates as device-under-test (DUT) on a bending fixture.

as dielectric and a self-aligned top electrode for precise control of capacitance [3], [4]. Other techniques like silver-based ink printing [5], [6], [7], [8], [9], liquid metal [1], [2], [3], [4], [5], [6], [7], [8], [9], [10], [11], [12], [13], and conducting polymer [14] have been explored for low-cost flexible microwave components including inductors, capacitors, and filters.

However, extensive use of non-degradable plastic and toxic materials in flexible electronics will generate an increasing amount of electronic waste as the large-scale deployment of flexible electronics-based devices like wearable devices. To the electronic waste issue of flexible electronics, cellulose nanofibril (CNF) substrate has been investigated due to its biodegradability and excellent properties at microwave frequency [2]. CNF substrate is derived from wood, which is not only biodegradable by fungi [15] but also can be manufactured at a very low cost due to abundant wood resources on earth. A recent report about the incineration of CNF substrate provides another way to dispose of CNF-based flexible substrate [16]. CNF substrates have demonstrated excellent mechanical flexibility and have been used as supporting substrates of flexible thin-film microwave devices, like transistors, diodes, and other components [15], [16], [17]. As critical components in microwave circuits, high-performance lumped spiral inductors, and metal-insulator-metal (MIM) capacitors have been developed on CNF substrates with acceptable electrical and mechanical performance. In this paper, we demonstrate high-performance flexible lumped passive components as well as flexible microwave filters on CNF substrate by optimizing the layout and fabrication processes of the filters. Instead of using TiO2 as dielectric material, polyimide which possesses a lower Young's modulus was used in our work. It simplified the fabrication process by getting rid of the oxide dielectric material deposition. The design technology co-optimization ensures good electrical performance, mechanical performance, and manufacturability. Due to the innovative use of polymer-based dielectric materials in MIM capacitors, the demonstrated filters can achieve a bending radius as small as 15 mm while maintaining excellent performance at microwave frequency.

II. DESIGN AND FABRICATION OF FLEXIBLE MICROWAVE COMPONENTS ON CNF SUBSTRATE

Before design and fabrication of flexible microwave components, a 200 μm thick epoxy coated-CNF thin film substrate was prepared, which was made from filtered, dried, and cured tetramethylpiperidine-1-oxy (TEMPO) oxidized wood pulp epoxy coated CNF films, as described previously [2], [18], [19]. The CNF substrate has a dielectric constant of 2.5 and tangent loss of 0.04 at 5 GHz [2], which is critical to achieving

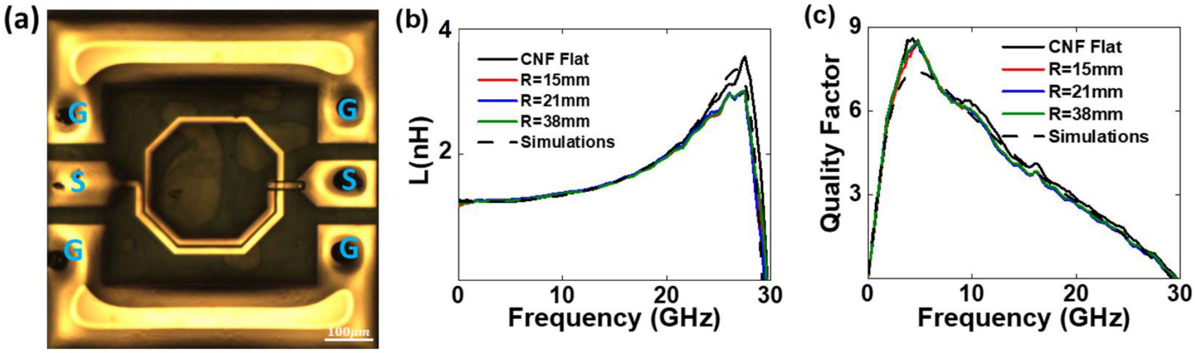

FIGURE 2. Measured 1.5-turn octagon spiral inductors on CNF with 15 μm line width and 5μm line spacing. (a) An optical microscopic image of the 1.5-turn octagon spiral inductor fabricated on CNF. (b) L values and (c) Q values were plotted as a function of frequency under flat and bending situations with a bending radius of 15 mm, 21 mm, and 38 mm, respectively. The simulation results of the inductors are also plotted as a comparison.

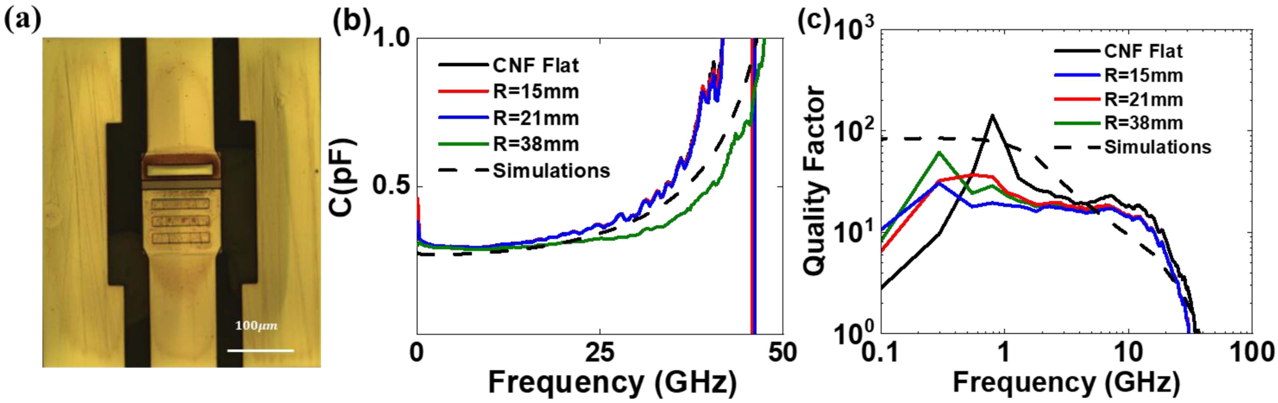

FIGURE 3. Measured 100 μm $\times$150 μm MIM capacitor on CNF. (a) An optical microscopic image of the 100 μm $\times$150 μm MIM capacitor fabricated on CNF. (b) C values and (c) Q values were plotted as a function of frequency under flat and bending situations with a bending radius of 15 mm, 21 mm, and 38 mm, respectively. The simulation results of the inductors are also plotted as a comparison.

low-loss passive microwave components like spiral inductors and filters.

The fabrication process flow of flexible spiral inductors (L), capacitors (C), and LC filters are schematically illustrated in Fig. 1. The process began with coating a thin layer (60 nm thick) of polymethylmethacrylate (950 PMMA A2) as a sacrificial layer on a Si substrate, which serves as a temporary rigid supporting substrate for following fabrication steps. Multiple layers of Polyimide (PI), with a total thickness of 13.2 μm, were subsequently coated on the temporary supporting substrate as shown in Fig. 1(a), followed by deposition of the first metal layer (M1) (Ti/Cu/Ti: 10 nm /980 nm /10 nm) using conventional metal lift-off process (Fig. 1(b)). This metal layer serves as connecting metal trace of spiral inductors and the bottom metal electrode of metal-insulator-metal (MIM) capacitors. The first metal layer was encapsulated by spin-coating a 1.35 μm thick PI layer (Fig. 1(c)). In addition to acting as an insulation layer between the first and second metal layers, the PI layer also acts as a dielectric layer of MIM capacitors, which replaces widely used inorganic oxide dielectric. Due to the low Young's modulus of PI (2.5Gpa) compared to most oxide dielectric (70-300GPa), the fabricated MIM capacitor can effectively reduce the strain of the dielectric layer and thus achieve a smaller bending radius, which is a key to achieving ultra-flexible microwave components [20]. Via holes for connecting the first and second metal layers were formed through the insulation PI layer by dry etching with a 100nm thick Al hard mask, as depicted in Fig. 1(d). After the via holes were formed, a second metal layer (M2) consisting of Ti/Cu/Ti (10 nm/1480 nm/10 nm) was deposited with photolithography and lift-off process. Since the M2 layer formed the spiral metal lines of the inductor, the top metal layer of the MIM capacitors, and the interconnect (also the RF probing pads) lines, thicker metal was used to reduce resistive loss and accordingly increase microwave performance of the components. The interconnect lines connect the inductor and the capacitor forming the LC-filters (Fig. 1(e)). After multiple optimizations using electron-magnetic simulation (Momentum in Keysight ADS), the M2 layer of spiral inductors was designed to have a width of 15 μm and spacing of 5 μm. The fabricated device on the supporting substrate consists of multiple inductors, capacitors,

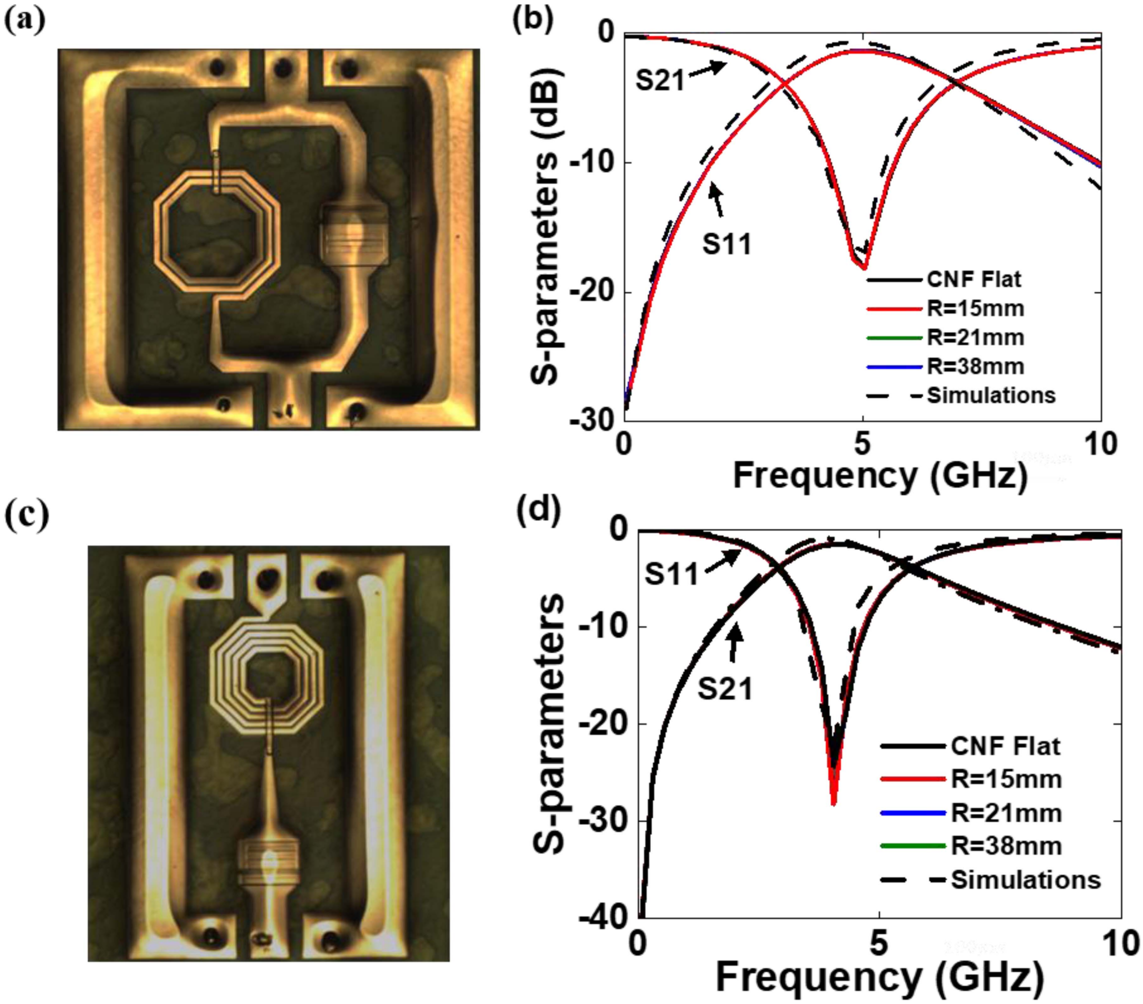

FIGURE 4. (a) An optical microscopic image of the CNF band-stop LC filter. (b) Measured S-parameters of a CNF 5-GHz band-stop L-C filter consisting of a 2.5-turn spiral inductor and a 100 μm $\times$150 μm MIM capacitor as a function of frequency under flat and bending situations with a bending radius of 15 mm, 21 mm, and 38 mm, respectively. The simulation results are plotted in the dashed lines for comparison. (c) An optical microscopic image of the CNF band-pass LC filter. (d) Measured S-parameters of a CNF 4-GHz band-pass L-C filter consisting of a 4.5-turn spiral inductor and a 100 μm $\times$150 μm MIM capacitor as a function of frequency under flat and bending situations with a bending radius of 15 mm, 21 mm, and 38 mm, respectively. The simulation results are plotted in the dashed lines for comparison.

and LC filters and was boiled in hot acetone to dissolve the sacrificial PMMA layer (Fig. 1(f)). Once the PMMA layer was fully dissolved, the device encapsulated in PI was weakly attached to the temporary Si substrate and can be easily picked up using a polydimethylsiloxane (PDMS) stamp (Fig. 1(g)). The membrane picked up by the PDMS stamp was then printed on a 200 μm thick CNF substrate with a partially cured SU-8 layer as the adhesive interface, using a modified MJB-3 contact aligner, as shown in Fig. 1(h). Fig. 1(i) shows schematic cross-section views of the device during each fabrication step illustrated in Fig. 1(a)–(h). The completed flexible inductors, capacitors, and LC filters on a transparent CNF substrate were shown in Fig. 1(j).

III. CHARACTERIZATION AND ANALYSIS

Direct current (DC) and radiofrequency (RF) performance of fabricated inductors, capacitors, and the LC-filters were characterized using Keysight 4200A SCS parameter analyzer and Agilent E8364A performance network analyzer, respectively, under different mechanical bending conditions. Inductance (L), capacitance (C), Self-resonant frequencies (f_{res}), and Q factors of the fabricated inductors and capacitance were extracted from the measured scattering parameters (S-parameters) using equations in

$$L = \frac{image\,(Z_{11})}{2\pi f}$$

$$C = -\frac{1}{2\pi f \times image\,(Z_{11})}$$

$$f_{res} = \frac{1}{2\pi\sqrt{LC}}$$

$$Q = \frac{2\pi f \times L}{Resistance} = \frac{1}{2\pi f \times C \times Resistance}.$$

Fig. 1(k) shows a photograph of the device during RF characterization under mechanical bending.

Fig. 2(a) shows a microscopic image of a 1.5-turn spiral inductor, which was characterized by different mechanical deformations. As shown in Fig. 2(b) and (c), the inductance and quality factor extracted from the measurement fit well with the simulation result on a flat CNF substrate. Fig. 2(b) and (c) indicate that f_{res} of the inductor reaches 29.8 GHz while achieving a Q factor as high as 8.5, which is the highest reported f_{res} of a flexible inductor based on our knowledge [3], [4]. The inductor can maintain constant inductance around 1.2 nH up to 10 GHz, which is important for achieving stable microwave performance over a wide band. More importantly, the inductor shows a negligible change in inductance and quality factor under different mechanical deformation. The negligible change of inductance and quality actor is possibly due to the narrow spacing of the metal trace in the spiral inductor, which prevents significant change of electromagnetic (EM) field distribution when the inductor is mechanically bent. The speculation was verified by EM simulations of the inductor under different mechanical deformations. The measured dc resistance of the 1.5 turn spiral inductor is 5 ohms, which significantly reduces resistive loss of the inductor.

Fig. 3 depicts the characterization of a flexible MIM capacitor with an area of 100 $\times$ 150 μm^2 under flat and bending conditions and compares with the simulation results. As shown in Figs. 3(b) and (c), the MIM capacitor presents a constant capacitance of 0.30 pF up to 25 GHz and 45 GHz f_{res}, which can be combined with the high-performance flexible inductor demonstrated in Fig. 2 to form wide-band high-frequency microwave circuits. Due to the use of low Young's modulus material (PI) as a dielectric layer, the MIM capacitor shows superior mechanical flexibility and exhibits stable RF performance with a bending radius as small as 15 mm.

Based on the high-performance spiral inductors and MIM capacitors, high-performance flexible band-stop, and band-pass filters with center frequencies of around 4–5 GHz, *i.e.,* the frequency band of Wi-Fi communications, were built on a CNF substrate. The band-stop filter was designed to consist of a 2.5 turn spiral inductor and a 100 $\times$ 150 μm^2 MIM capacitor in shunt connection as depicted in Fig. 4(a). Fig. 4(b) compares the measured insertion loss (S21) and return loss (S11) of the band-stop filter under flat and different bending conditions along with the simulation results on a flat CNF substrate for comparison. The filter operates around 5 GHz as designed, with an insertion loss of more than 18.2 dB and a return loss of less than 1.3 dB at 5.04 GHz. Due to the excellent mechanical stability of the MIM capacitor and spiral inductor, the filter shows a negligible difference in insertion loss and return loss under different mechanical deformations. The band-pass filter was configured using a serially connected 4.5 turn spiral inductor and 100 $\times$ 150 μm^2 MIM capacitor, as shown in Fig. 4(c). The filter shows more than 28 dB insertion loss and smaller than 1.4 dB return loss at 4 GHz as in Fig. 4(d). Same as the band-stop filter, the band-pass filter also exhibits negligible changes under different bending situations and fits the simulation excellently.

Supplementary Figure 1–3 presents the performance of intrinsic flexible inductor, capacitor, and filters after de-embedding pad parasitic using EM simulation-based dummy open and short patterns. The excellent mechanical robustness and high RF performance obtained on the spiral inductors, MIM capacitors, and filters indicate that its CNF substrate is a good candidate for future complex flexible microwave circuits operating up to 10 GHz. Moreover, the reliable fabrication process can be easily applied to achieve other complex circuits like the wide band-pass filter shown in Supplementary Figure 4.

IV. CONCLUSION

We demonstrated high-performance compact spiral inductors, MIM capacitors, and LC-based RF filters on flexible CNF substrates. Record-high resonance frequencies of 29.8 GHz and 45 GHz were achieved from a 1.5-turn spiral inductor and a MIM capacitor, respectively. The return loss of the demonstrated LC-based band-stop filter is higher than 18.2dB and insertion losses of the band-pass filter are less than 1.4 dB, respectively. These high-performance flexible microwave components on CNF substrate prove that CNF substrate is an excellent flexible substrate for a wide range of microwave circuit applications, which will be a critical component for future complex flexible microwave electronics.

REFERENCES

[1] H. Zhang et al., "Flexible and stretchable microwave electronics: Past, present, and future perspective," *Adv. Mater. Technol.*, vol. 6, no. 1, 2021, Art. no. 2000759.

[2] H. Mi et al., "Characterizations of biodegradable epoxy-coated cellulose nanofibrils (CNF) thin film for flexible microwave applications," *Cellulose*, vol. 23, no. 3, pp. 1989–1995, 2016.

[3] L. Sun et al., "Flexible high-frequency microwave inductors and capacitors integrated on a polyethylene terephthalate substrate," *Appl. Phys. Lett.*, vol. 96, no. 1, 2010, Art. no. 013509.

[4] S. J. Cho, Y. H. Jung, and Z. Ma, "X-band compatible flexible microwave inductors and capacitors on plastic substrate," *IEEE J. Electron Devices Soc.*, vol. 3, no. 5, pp. 435–439, Sep. 2015.

[5] H. Lee, M. M. Tentzeris, P. Markondeya, M. K. P. Raj, and Y. Kawahara, "Inkjet-printed ferromagnetic nanoparticles for miniaturization of flexible printed RF inductors," in *Proc. IEEE Antennas Propag. Soc. Int. Symp.*, 2013, pp. 994–995.

[6] H. Lee, B. S. Cook, K. P. Murali, M. Raj, and M. M. Tentzeris, "Inkjet printed high-Q RF inductors on paper substrate with ferromagnetic nanomaterial," *IEEE Microw. Wireless Compon. Lett.*, vol. 26, 2016, Art. no. 419

[7] A. Menicanin, L. Živanov, Č. Žlebič, M. Kisić, N. Blaž, and M. Damnjanović, "Fully inkjet printed CPW meander inductors on PET flexible substrate," in *Proc. Int. Spring Semin. Electron. Technol.*, 2015, pp. 43–46.

[8] A. B. Menicanin, L. D. Zivanov, M. S. Damnjanovic, and A. M. Maric, "Low-cost CPW meander inductors utilizing ink-jet printing on flexible substrate for high-frequency applications," *IEEE Trans. Electron Devices*, vol. 60, 2013, Art. no. 827.

[9] W. Chen, Y. Li, R. Li, A. V. -Y. Thean, and Y. -X. Guo, "Bendable and stretchable microfluidic liquid metal-based filter," *IEEE Microw. Wireless Compon. Lett.*, vol. 28, no. 3, pp. 203–205, Mar. 2018, doi: 10.1109/LMWC.2018.2799382.

[10] B. S. Cook, J. R. Cooper, and M. M. Tentzeris, "Multi-layer RF capacitors on flexible substrates utilizing inkjet printed dielectric polymers," *IEEE Microw. Wireless Compon. Lett.*, vol. 23, 2013, Art. no. 353.

[11] B. S. Cook et al., “Inkjet-printed, vertically-integrated, high-performance inductors and transformers on flexible LCP substrate,” in *Proc. IEEE MTT-S Int. Microw. Symp.*, 2014, pp. 1–4.

[12] C. Mariotti, F. Alimenti, L. Roselli, and M. M. Tentzeris, “High-performance RF devices and components on flexible cellulose substrate by vertically integrated additive manufacturing technologies,” *IEEE Trans. Microw. Theory Techn.*, vol. 65, 2017, Art. no. 62.

[13] C. Mariotti, B. S. Cook, F. Alimenti, L. Roselli, and M. M. Tentzeris, “Additively manufactured multilayer high performance RF passive components on cellulose substrates for Internet-of-Things electronic circuits,” in *Proc. IEEE MTT-S Int. Microw. Symp.*, 2015, pp. 1–4.

[14] I. Cherukhin, S. P. Gao, and Y. Guo, “Fully flexible polymer-based microwave devices: Materials, fabrication technique, and application to transmission lines,” *IEEE Trans. Antennas Propag.*, vol. 69, no. 12, pp. 8763–8777, Dec. 2021.

[15] Y. H. Jung et al., “High-performance green flexible electronics based on biodegradable cellulose nanofibril paper,” *Nature Commun.*, vol. 6, no. 1, pp. 1–11, 2015.

[16] H. Zhang et al., “Heterogeneously integrated flexible microwave amplifiers on a cellulose nanofibril substrate,” *Nature Commun.*, vol. 11, no. 1, pp. 1–11, 2020.

[17] S. Rezania et al., “Microplastics pollution in different aquatic environments and biota: A review of recent studies,” *Marine Pollut. Bull.*, vol. 133, pp. 191–208, 2018.

[18] H. A. Khalil, A. H. Bhat, and A. I. Yusra, “Green composites from sustainable cellulose nanofibrils: A review,” *Carbohydrate Polymers*, vol. 87, no. 2, pp. 963–979, 2012.

[19] Y. Qing, R. Sabo, Z. Cai, and Y. Wu, “Resin impregnation of cellulose nanofibril films facilitated by water swelling,” *Cellulose*, vol. 20, no. 1, pp. 303–313, 2013.

[20] Z. Suo, E. Y. Ma, H. Gleskova, and S. Wagner, “Mechanics of rollable and foldable film-on-foil electronics,” *Appl. Phys. Lett.*, vol. 74, no. 8, pp. 1177–1179, 1999.